

# NLO DGLAP splitting kernels for color non-singlet DPDs

Florian Fabry – [florian.fabry@desy.de](mailto:florian.fabry@desy.de)

Deutsches Elektronen-Synchrotron, DESY

work in collaboration with Markus Diehl and Alexey Vladimirov

[MPI@LHC workshop 2022](#)

November 17, 2022

**HELMHOLTZ**

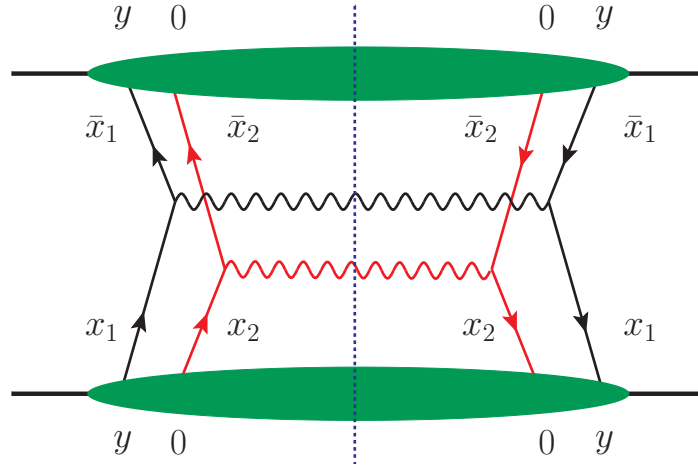


# Setting the stage

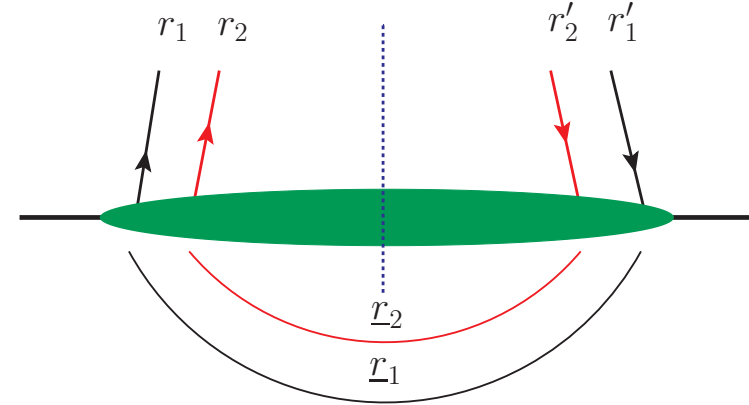
---

- Color non-singlet DPDs suppressed by Sudakov factor ([Artru, Mekhfi; 1988], [Manohar, Waalewijn; 2012])
  - rapidity dependence, see later
- Also suppressed after DGLAP evolution?  
**Not necessarily!** (see previous talk, [Blok, Mehl; 2022])
- Until now, DGLAP evolution available only at LO...
- Let's go to **NLO!**

# Double parton distributions (DPDs)



LO double Drell-Yan production  
adapted from [Diehl, Gaunt; 2017]



DPD color indices  
adapted from [Diehl, Gaunt; 2017]

Matrix element structure very similar to the one of PDFs:

$$F_{a_1 a_2}^{r_1 r_2}(x_i, \mathbf{y}, \mu_i, \zeta) \propto \int dy^- \frac{dz_1^-}{2\pi} \frac{dz_2^-}{2\pi} e^{i(x_1 z_1^- + x_2 z_2^-)p^+} \\ \times \langle p | \mathcal{O}_{a_1}^{r_1}(y, z_1, \mu_1, \zeta) \mathcal{O}_{a_2}^{r_2}(0, z_2, \mu_2, \zeta) | p \rangle \Big|_{y^+ = z_1^+ = z_2^+ = 0, z_1 = z_2 = 0}$$

Operators inside matrix element have the same structure as the ones inside PDFs

# DGLAP evolution of DPDs

- Collinear,  $y$ -dependent DPDs evolve with a DGLAP equation

$$\frac{d}{d \ln \mu_1} R_1 R_2 F_{a_1 a_2}(x_i, \mu_i, \zeta) = 2 \sum_{b, R'} R_1 \bar{R}' P_{a_1 b}(x'_1, \mu_1, x_1^2 \zeta) \otimes_{x_1} R' R_2 F_{b a_2}(x_1, x_2, \mu_i, \zeta)$$

(analoguous equation for  $\mu_2$ )

Note: finite distance  $y$  acts as a UV-cutoff for otherwise existing divergences in interactions between the two partons

- Diagonal after projection onto irreducible representations with the help of color projector:

$$R_1 R_2 F_{a_1 a_2} \propto P_{\bar{R}_1 \bar{R}_2}^{r_1 r_2} F_{a_1 a_2}^{r_1 r_2} \begin{matrix} \rightarrow 3 \otimes \bar{3} = 1 \oplus 8 \\ \rightarrow 8 \otimes 8 = 1 \oplus 8_A \oplus 8_S \oplus 10 \oplus \bar{10} \oplus 27 \end{matrix}$$

- New feature: **rapidity dependence!**

# Rapidity dependence of DPDs

- Rapidity divergences compensated by a soft factor, same structure as for TMDs!
- Rapidity dependence in DPDs:

$$\frac{\partial}{\partial \ln \zeta} {}^{R_1 R_2} F_{a_1 a_2}(x_i, \mathbf{y}; \mu_i, \zeta) = \frac{1}{2} {}^{R_1} J(\mathbf{y}; \mu_i) {}^{R_1 R_2} F_{a_1 a_2}(x_i, \mathbf{y}; \mu_i, \zeta)$$

- Rapidity dependence in splitting kernels:

$$\frac{\partial}{\partial \ln \zeta} {}^{R R'} P_{ab}(x, \mu_1, \zeta) = -\frac{1}{4} \delta_{R \bar{R}'} \delta_{ab} \delta(1-x) {}^R \gamma_J(\mu)$$

→ additional rapidity term in color non-singlet splitting kernels,

for color singlet:  ${}^1 J = 0$ ,  ${}^1 \gamma_J = 0$

# Sudakov factor inside DPDs

- Isolate ( $x$ -independent) rapidity dependence:

$$\begin{aligned}
 & R_1 R_2 F_{a_1 a_2}(x_i, \mathbf{y}; \mu_i, \zeta) \\
 &= \exp \left[ R_1 J(\mathbf{y}, \mu_i) \log \frac{\sqrt{\zeta}}{\mu_y} + \int_{\mu_y}^{\mu_1} \frac{d\mu}{\mu} R_1 \gamma_J(\mu) \log \frac{\mu}{\mu_y} + (\mu_1 \leftrightarrow \mu_2) \right] \\
 &\times \hat{F}_{a_1 a_2, \mu_0, \mu_y^2}(x_i, \mathbf{y}; \mu_i), \quad \mu_y = \frac{2e^{-\gamma_E}}{y^*}, \quad \zeta \sim \mathcal{O}(Q)
 \end{aligned}$$

See talk by Peter Plößl

- Let's get an idea of the effect of the Sudakov factor. Expand only to LO and use RGE of CS kernel. The last term determines behavior.


$$\exp \left[ R_1 J(\mu_y, \mu_y) \log \frac{\sqrt{\zeta}}{\mu_y} + \frac{\pi R_1 \gamma_J^{(0)}}{\beta_0} \sum_{i=1,2} \left( \log \frac{\mu_i}{\mu_y} - \left[ \log \log \frac{\mu_i}{\Lambda} - \log \log \frac{\mu_y}{\Lambda} \right] \log \frac{\sqrt{\zeta}}{\Lambda} \right) \right]$$

Logs inside CS kernel vanish at this scale configuration.   
 Vanishes for color singlet   
 Suppression!   
 Vanishes for  $\mu_y = \mu_i \rightarrow$  **no/weak suppression** at certain scales! (see also [Blok, Mehl; 2022])

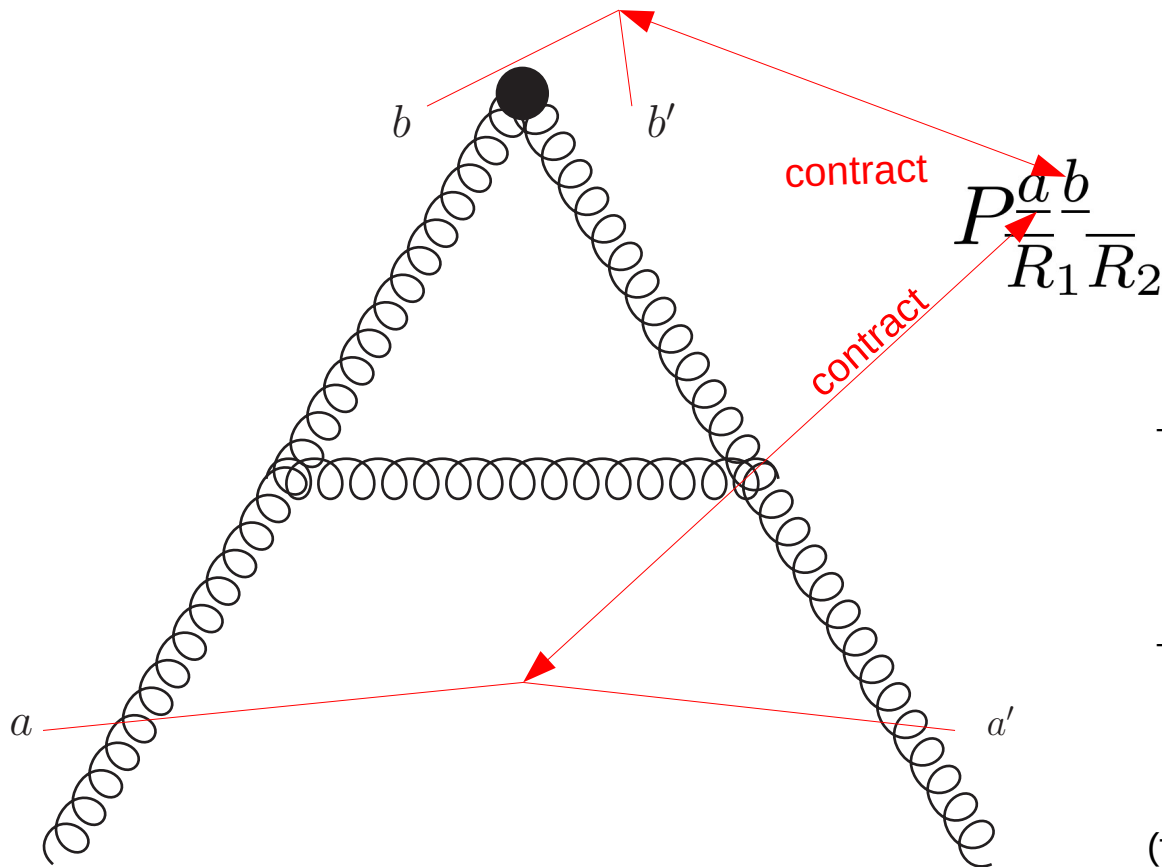
# Sudakov factor inside DPDs

- Main takeaway: Sudakov suppression can be small/absent!
- Thus, understanding effect of remaining (x-dependent) log and DGLAP evolution becomes even more important.
- DGLAP equation for “reduced” DPD:

$$\begin{aligned}
 & \frac{\partial}{\partial \log \mu_1} R_1 R_2 \hat{F}_{a_1 a_2, \mu_0, \zeta_0}(x_1, x_2, \mathbf{y}; \mu_1, \mu_2) \quad \text{absent in color singlet} \\
 &= - R_1 \gamma_J(\mu_1) \log x_1 R_1 R_2 \hat{F}_{a_1 a_2, \mu_0, \zeta_0}(x_1, x_2, \mathbf{y}; \mu_1, \mu_2) \\
 &+ 2 \sum_{b_1, R'_1} R_1 \bar{R}'_1 P_{a_1 b_1}(x'_1; \mu_1, \mu_1^2) \otimes_{x_1}^{R'_1 R_2} \hat{F}_{b_1 a_2, \mu_0, \zeta_0}(x'_1, x_2, \mathbf{y}; \mu_1, \mu_2)
 \end{aligned}$$


 No x-dependence in rapidity variable, Mellin convolution as we know it

# LO colored DGLAP kernels



→ Leads to a global “color” factor for all non- $\delta(1-x)$  terms:

$$R_1 R_2 P_{ab}^{(0)}(x) = c_{ab} (R_1 R_2)^{11} P_{ab}^{(0)}(x)$$

→  $\delta(1-x)$  terms stay as they are, because color projectors are normalized to unity

(first done in [Diehl, et. al.; 2011], also used in [Blok, et.al.; 2022])

# NLO colored DGLAP kernels

---

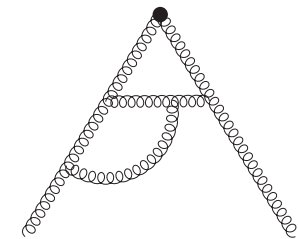
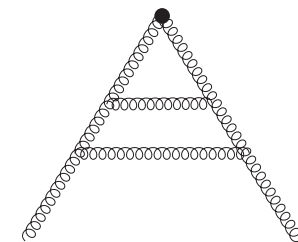
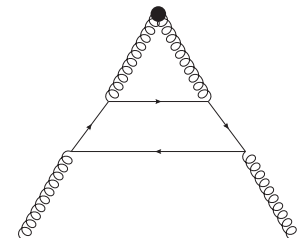
- More graphs  $\rightarrow$  more color factors  $\rightarrow$  no global factor, but more involved structure!
- Need to regulate rapidity divergencies
- Calculated using two methods:
  1. Based on **existing results of DGLAP kernels for PDFs**
  2. Based on **short distance matching of TMD operators** projected onto color non-singlet representations

# 1. Method: Extraction from graph-by-graph results

*based on [Curci, Furmanski, Petronzio; 1980], [Ellis, Vogelsang; 1996],  
[Vogelsang; 1996] and [Vogelsang; 1997]  
(special thanks to Werner Vogelsang for help)*

# Approach

Terms				
	(b <sub>q</sub> )	(b <sub>g</sub> )	(c)	(d)
$p_{gg}(x) \ln^2(x)$		-2	4	
$p_{gg}(x) \ln^2(1-x)$			4	
$p_{gg}(x) \ln(x) \ln(1-x)$			16	
$p_{gg}(x) I_0(\ln(1-x) + \ln(x))$			24	
$p_{gg}(x) \ln(x)$			-22/3	4/3
...		...		



(tables based on results from the publications on the previous slide)

# Approach

Combine with

$RR'$	11	$AA$	$SS$	27 27
global factor	1	1	1	1
graph (b <sub>q</sub> )	$-\frac{1}{2N}n_f$	0	$-\frac{1}{N}n_f$	$\frac{1}{2}n_f$
graph (b <sub>g</sub> )	$\frac{N^2}{2}$	0	0	$\frac{5}{2}$
graph (c)	$\frac{N^2}{2}$	$\frac{1}{4}N^2$	$\frac{1}{4}N^2$	$-\frac{3}{2}$
graph (d)	$\frac{N}{2}n_f$	$\frac{1}{4}Nn_f$	$\frac{1}{4}Nn_f$	$-\frac{1}{2}n_f$
...			...	

*(need to recalculate 4-gluon vertex diagrams from scratch)*

# Limitations: the rapidity dependence

---

- Calculational method tailored for collinear PDFs
  - No sensitivity to rapidity divergences,  
i.e. no extraction of  $\delta(1-x)$  terms possible
- Either invent new scheme that also regulates rapidity divergences,  
or make use of existing literature
  - **TMD matrix elements!**
- *serves also a cross check for all the non- $\delta(1-x)$  terms*

## 2. Method: Extraction from projected TMD matrix elements

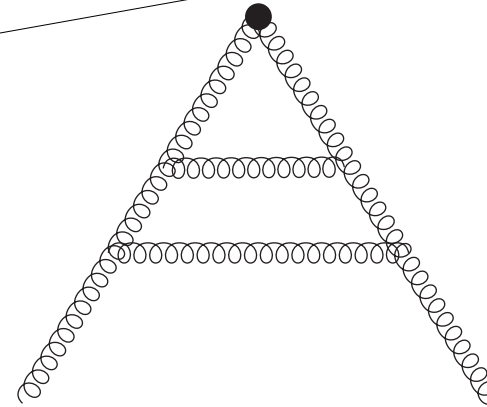
*based on [Echevarria, Scimemi, Vladimirov; 2016]  
and [Gutierrez-Reyes, Scimemi, Vladimirov; 2018]*

# Approach

Use short distance matching formula between collinear PDF and TMD matrix elements to have access to rapidity regulator.

$${}^{RR'}\widehat{\mathcal{M}}_{ab}(x, z, \mu, \zeta) = \sum_{c, R''} {}^{R\bar{R}''}C_{ac}(x', z, \mu, x^2\zeta) \otimes_x {}^{R''R'}\mathcal{M}_{cb}(x', \mu, \zeta)$$

again obtained from evaluating  
color projected diagrams like



*Extract splitting kernels from single pole at NNLO after calculating the matrix elements up to desired order.*

# Results

- Kernels can be decomposed such that

$${}^{RR'}P_{ab}(x, \zeta_p/\mu^2) = \underline{{}^{RR'}P_{ab,\text{real}}(x)} + \left( \delta_{R\bar{R}'}\delta_{ab}P_{a,\text{sing}} + \underline{{}^{RR'}P_{ab,\text{non-sing}}} - \frac{1}{4}\delta_{R\bar{R}'}\delta_{ab}\underline{{}^R\gamma_J} \ln \frac{\zeta_p}{\mu^2} \right) \delta(1-x)$$

- **Part from real graphs** calculated with both methods
- Casimir scaling of NLO **anomalous dimension** same as at LO!

$${}^{10}\gamma_J^{(1)} = {}^{\overline{10}}\gamma_J^{(1)} = 2 {}^8\gamma_J^{(1)} \Big|_{N=3} = 134 - 6\pi^2 - \frac{20}{3}n_f,$$
$${}^{27}\gamma_J^{(1)} = \frac{8}{3} {}^8\gamma_J^{(1)} \Big|_{N=3}.$$

- Identical Casimir scaling also for the **additional “non-sing” terms**

# Summary

---

- For the first time, obtained all colored NLO DGLAP kernels, for unpolarized, longitudinal and transversity distributions
- All non- $\delta(1-x)$  terms are cross-checked with two completely independent methods
- Also obtained the NLO anomalous dimension of the CS-kernel for higher-than-octet representations

*Stay tuned for numerical results!*

Thank you for your attention!

# Back up: Color Projectors

$$P_{11}^{ab} = \frac{1}{N^2 - 1} \delta^{aa'} \delta^{bb'}$$

$$P_{AA}^{ab} = \frac{1}{N} f^{aa'c} f^{bb'c}$$

$$P_{SS}^{ab} = \frac{N}{N^2 - 4} d^{aa'c} d^{bb'c}$$

$$P_{AS}^{ab} = \frac{1}{\sqrt{N^2 - 4}} f^{aa'c} d^{bb'c}$$

$$P_{SA}^{ab} = \frac{1}{\sqrt{N^2 - 4}} d^{aa'c} f^{bb'c}$$

$$P_{10\overline{10}}^{ab} = \frac{1}{4} \left( \delta^{ab} \delta^{a'b'} - \delta^{ab'} \delta^{a'b} \right) - \frac{1}{2} P_{AA}^{ab} - \frac{i}{4} \left( d^{abc} f^{a'b'c} + f^{abc} d^{a'b'c} \right)$$

$$P_{\overline{10}10}^{ab} = \frac{1}{4} \left( \delta^{ab} \delta^{a'b'} - \delta^{ab'} \delta^{a'b} \right) - \frac{1}{2} P_{AA}^{ab} + \frac{i}{4} \left( d^{abc} f^{a'b'c} + f^{abc} d^{a'b'c} \right)$$

$$P_{27\overline{27}}^{ab} = \frac{1}{2} \left( \delta^{ab} \delta^{a'b'} + \delta^{ab'} \delta^{a'b} \right) - P_{SS}^{ab} - P_{11}^{ab}$$

# DGLAP evolution channels

---

- Color singlet: Identical splitting kernels as for PDFs
- Two flavor-singlet combinations in the color octet:
  - $\sum_{q=u,d,s,\dots} \left( {}^8q + {}^8\bar{q} \right)$  mixes with symmetric gluon
  - $\sum_{q=u,d,s,\dots} \left( {}^8q - {}^8\bar{q} \right)$  mixes with antisymmetric gluon
- Gluon decuplet and 27-multiplet evolve independently from quark distributions







# Backup: Flavor singlet evolution equations

- Two flavor-singlet combinations in the color octet:

$$\frac{d}{d \ln \mu_1} \begin{pmatrix} R_1 R_2 F_{\Sigma^+ a_2} \\ R_3 R_4 F_{ga_4} \end{pmatrix} = 2 \begin{pmatrix} R_1 R_1 P_{\Sigma^+ \Sigma^+} & n_f R_1 R_3 P_{\Sigma^+ g} \\ R_3 R_1 P_{g \Sigma^+} & R_3 R_3 P_{gg} \end{pmatrix} \otimes_{x_1} \begin{pmatrix} R_1 R_2 F_{\Sigma^+ a_2} \\ R_3 R_4 F_{ga_4} \end{pmatrix}, \quad R_1 R_3 = 11, 8S$$

$$\frac{d}{d \ln \mu_1} \begin{pmatrix} 8R_2 F_{\Sigma^- a_2} \\ AR_4 F_{ga_4} \end{pmatrix} = 2 \begin{pmatrix} 88P_{\Sigma^- \Sigma^-} & n_f 8A P_{\Sigma^- g} \\ A8P_{g \Sigma^-} & AA P_{gg} \end{pmatrix} \otimes_{x_1} \begin{pmatrix} 8R_2 F_{\Sigma^- a_2} \\ AR_4 F_{ga_4} \end{pmatrix}$$

# Backup: Method overview

	Unpol.	Longit./ Helicity	Transv.
Method 1: Graphs			
Method 2: Matching			

Matrix elements not available to us in the form we need

# Backup: Longitudinal kernels: scheme change

$\gamma_5$  matrix does not anti-commute with all  $\gamma$  matrices in dim. reg. with more than 4 space-time dimension.

- This leads to additional terms that violate scale independence of a combination of non-singlet distributions (see [Vogelsang; 1996]).
- Get rid of these terms with a scheme change on twist-2 operator level:

$${}^R\mathcal{O}_{\Delta q_i} = {}^R\tilde{Z} \otimes {}^R\mathcal{O}_{\Delta q_i, \overline{\text{MS}}}$$

$${}^R\mathcal{O}_{\Delta \bar{q}_i} = {}^R\tilde{Z} \otimes {}^R\mathcal{O}_{\Delta \bar{q}_i, \overline{\text{MS}}}$$

This leads to:

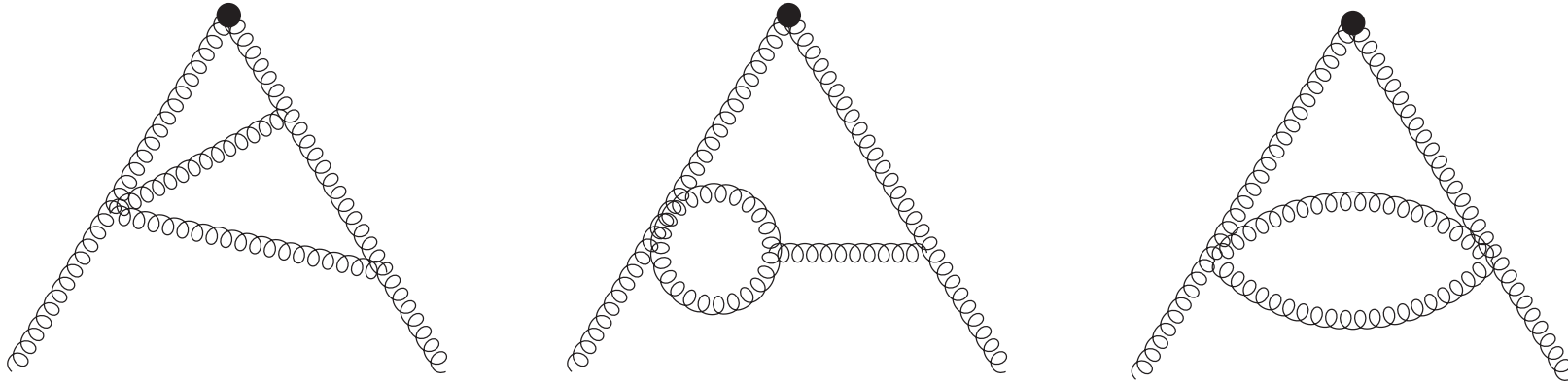
$${}^{RR}P_{\Delta}^{\pm, (0)} = {}^{RR}P_{\Delta, \overline{\text{MS}}}^{\pm, (0)}$$

$${}^{RR}P_{\Delta}^{\pm, (1)} = {}^{RR}P_{\Delta, \overline{\text{MS}}}^{\pm, (1)} - \frac{1}{2}\beta_0 {}^R\tilde{Z}^{(1)}$$

$${}^{RR'}P_{\Delta\Sigma^{\pm}\Delta g}^{(1)} = {}^{RR'}P_{\Delta\Sigma^{\pm}\Delta g, \overline{\text{MS}}}^{(1)} + {}^R\tilde{Z}^{(1)} \otimes {}^{RR'}P_{\Delta\Sigma^{\pm}\Delta g}^{(0)}$$

$${}^{R'R}P_{\Delta g\Delta\Sigma^{\pm}}^{(1)} = {}^{R'R}P_{\Delta g\Delta\Sigma^{\pm}, \overline{\text{MS}}}^{(1)} - {}^{R'R}P_{\Delta g\Delta\Sigma^{\pm}}^{(0)} \otimes {}^R\tilde{Z}^{(1)}$$

# What about 4-vertex graphs?



Color structure of gluon 4-vertex does not factorize:

$$\begin{aligned} & f^{e'bc} f^{e'ea} \left( g^{\nu'\beta'} g^{\mu\alpha'} - g^{\nu'\mu} g^{\alpha'\beta'} \right) \\ & + f^{e'be} f^{e'ca} \left( g^{\nu'\alpha'} g^{\beta'\mu} - g^{\nu'\mu} g^{\alpha'\beta'} \right) \\ & + f^{e'ba} f^{e'ce} \left( g^{\nu'\alpha'} g^{\beta'\mu} - g^{\nu'\beta'} g^{\mu\alpha'} \right) \end{aligned}$$

*Calculate by hand, using the methods illustrated in [Ellis, Vogelsang; 1996]*

# Calculating 4-vertex graphs

Master formula:

$${}^{RR'}\Gamma_{(k)}(x) = \text{PP} \left\{ \frac{1}{D-2} \int_0^{Q^2} d|k^2| \int dP S^{(2)} \frac{\mathcal{N}_{(k)}^{RR'}(x)}{2|k^2|^2} \right\}$$

prop. to splitting kernel

extracts single pole of  
expansion in  $\epsilon$

Integral over momentum flowing  
out of the top of the graph  
→ upper cut-off at hard scale

Graph with integral over  
residual phase space

- Equivalent to taking the UV part of the graph (scaleless integrals vanish in dim. reg.)
  - Splitting kernels as anomalous dimensions connected to renormalisation factors of PDF/DPD operators
  - See [Collins, Rogers, Sate; 2021] for a comparison of both approaches

# Method 2: Approach

- Make use of short distance matching formula between collinear PDF and TMD matrix elements to have access to rapidity regulator:

$${}^{RR'}\widehat{\mathcal{M}}_{ab}(x, z, \mu, \zeta) = \sum_{c, R''} {}^{R\bar{R}''}C_{ac}(x', z, \mu, x^2\zeta) \otimes_x {}^{R''R'}\mathcal{M}_{cb}(x', \mu, \zeta)$$

- R.h.s. calculated with the help of the  $\delta$ -regulator inside Wilson line  
[Echevarria et. al.]:

$$W_{rs}(\xi, v) = \mathcal{P} \exp \left\{ -ig t_{rs}^b \int_0^\infty ds v \cdot A^b(\xi + sv) e^{-\delta^+ s} \right\}$$

in eikonal propagators: 
$$\frac{1}{(k_1^+ - i\delta^+)(k_2^+ - 2i\delta^+) \dots (k_n^+ - ni\delta^+)}$$

# Method 2: Limitations(?)

- Colored matrix elements only available for unpol. and transv. case
  - $\delta(1-x)$  terms are missing for longitudinal kernels
- **However**, these terms come from kinematical regions in which gluons become soft → interaction can be approximated by eikonal coupling, which is **spin independent**
- This is validated
  - ... for all polarizations in color singlet case
    - known for a long time in the literature
  - ... for unpol. and transv. in all color representations (our results)

# Back up: Kernels in their full glory

$${}^{88}P_{qq}^{V,(1)}(x) = c_{qq}(88) \left\{ {}^{11}P_{qq}^{V,(1)}(x) - \frac{C_F C_A}{4} \left[ \left( 2p_{qq}(x) - (1+x) \right) \ln^2(x) \right. \right. \\ \left. \left. + (8-4x) \ln(x) + 6(1-x) \right] \right\}$$

$${}^{88}P_{q\bar{q}}^{V,(1)}(x) = (N^2 + 1) c_{qq}(88) {}^{11}P_{q\bar{q}}^{V,(1)}(x)$$

$${}^{88}P_{qq}^{S,(1)}(x) = -c_{qq}(88)(N^2 - 2) {}^{11}P_{qq}^{S,(1)}(x)$$

$${}^{88}P_{q\bar{q}}^{S,(1)}(x) = 2c_{qq}(88) {}^{11}P_{q\bar{q}}^{S,(1)}(x)$$

# Back up: Kernels in their full glory

$$\begin{aligned} {}^8A P_{\Sigma^-g}^{(1)}(x) = c_{qg}(8A) \Bigg\{ & {}^{11}P_{\Sigma^+g}^{(1)}(x) + \frac{1}{2}C_A \left[ \left( 3x - p_{\Sigma^\pm g}(x) + \frac{3}{2} \right) \ln^2(x) \right. \\ & + \frac{1}{3} \left( -89x - 22p_{\Sigma^\pm g}(x) + 4 \right) \ln(x) + \frac{109}{9} p_{\Sigma^\pm g}(x) \\ & \left. - 2S_2(x)p_{\Sigma^\pm g}(-x) + \frac{83}{9}x - \frac{172}{9} - \frac{20}{9x} \right] \Bigg\} \end{aligned}$$

$${}^8S P_{\Sigma^+g}^{(1)}(x) = \frac{c_{qg}(8S)}{c_{qg}(8A)} {}^8A P_{\Sigma^-g}^{(1)}(x)$$

# Back up: Kernels in their full glory

$$A8P_{g\Sigma^-}^{(1)}(x) = c_{gq}(A8) \left\{ {}^{11}P_{g\Sigma^+}^{(1)}(x) + \frac{C_F C_A}{18} \left[ -\left(\frac{27}{2}x + 9p_{g\Sigma^\pm}(x) + 27\right) \ln^2(x) \right. \right. \\ \left. \left. + \left(24x^2 + 27x + 135\right) \ln(x) + 58p_{g\Sigma^\pm}(x) \right. \right. \\ \left. \left. - 18S_2(x)p_{g\Sigma^\pm}(-x) - 44x^2 - 58x + 44 \right] \right\}$$

$$S8P_{g\Sigma^+}^{(1)}(x) = \frac{c_{gq}(S8)}{c_{gq}(A8)} A8P_{g\Sigma^-}^{(1)}(x)$$

# Back up: Kernels in their full glory

---

$$\begin{aligned} {}^{AA}P_{gg}^{(1)}(x) = c_{gg}(AA) & \left\{ C_A^2 \left[ 2(1+x) \ln^2(x) - 4p_{gg}(x) \ln(x) \ln(1-x) \right. \right. \\ & + \frac{1}{3} \left( -22x^2 + 14x - 4 \right) \ln(x) \\ & + \left. \frac{1}{9} \left( 67 - 3\pi^2 \right) p_{gg}(x) + 6(1-x) \right] \\ & + C_A n_f \left[ -\frac{1}{2} (1+x) \ln^2(x) - \frac{1}{6} \left( 19x + 13 \right) - \frac{10}{9} p_{gg}(x) \right. \\ & + \left. \left. \frac{28}{9} x^2 + x - 3 - \frac{10}{9x} \right] \right\} \end{aligned}$$

# Back up: Kernels in their full glory

---

$$\begin{aligned} {}^{SS}P_{gg}^{(1)}(x) &= \frac{c_{gg}(SS)}{c_{gg}(AA)} {}^{AA}P_{gg}^{(1)}(x) \\ &\quad + c_{gg}(SS) \left( \frac{1}{2} C_A - C_F \right) n_f \left\{ (1+x) \ln^2(x) + (5x+3) \ln(x) \right. \\ &\quad \left. - \frac{10}{3} x^2 - 4x + 8 - \frac{2}{3x} \right\} \end{aligned}$$

$${}^{AS}P_{gg}^{(1)}(x) = {}^{SA}P_{gg}^{(1)}(x) = 0$$

$${}^{10\overline{10}}P_{gg}^{(1)}(x) = {}^{\overline{10}10}P_{gg}^{(1)}(x) = 0$$

# Back up: Kernels in their full glory

$$\begin{aligned} {}^{27}{}^{27}P_{gg}^{(1)}(x) = c_{gg}(27\ 27) & \left\{ \left[ -15p_{gg}(x) - 12(1+x) \right] \ln^2(x) - 36p_{gg}(x) \ln(x) \ln(1-x) \right. \\ & + \left[ 44x^2 + 57x + 93 \right] \ln(x) - \left[ 3\pi^2 - 67 \right] p_{gg}(x) \\ & - 30S_2(x)p_{gg}(-x) - \frac{335}{3}x^2 - \frac{117}{2}(1-x) + \frac{335}{3x} \\ & \left. + n_f \left[ -2(1+x) \ln(x) - \frac{10}{3}p_{gg}(x) + \frac{13}{3}x^2 + 3(1-x) - \frac{13}{3x} \right] \right\} \end{aligned}$$

# Back up: Kernels in their full glory

$${}^{RR'}P_{ab}(x, \zeta_p/\mu^2) = {}^{RR'}P_{ab,\text{real}}(x) + \left( \delta_{R\bar{R}'} \delta_{ab} P_{a,\text{sing}} + {}^{RR'}P_{ab,\text{non-sing}} - \frac{1}{4} \delta_{R\bar{R}'} \delta_{ab} {}^R\gamma_J \ln \frac{\zeta_p}{\mu^2} \right) \delta(1-x).$$

$$\begin{aligned} {}^{88}P_{qq,\text{non-sing}}^{V,(1)} &= {}^{AA}P_{gg,\text{non-sing}}^{(1)} = {}^{SS}P_{gg,\text{non-sing}}^{(1)} \\ &= C_A^2 \left\{ \frac{101}{54} - \frac{11}{144} \pi^2 - \frac{7}{4} \zeta_3 \right\} + C_A n_f \left\{ \frac{1}{72} \pi^2 - \frac{7}{27} \right\} \end{aligned}$$

$$\begin{aligned} {}^{10\bar{10}}P_{gg,\text{non-sing}}^{(1)} &= {}^{\bar{10}10}P_{gg,\text{non-sing}}^{(1)} = 2 {}^{AA}P_{gg,\text{non-sing}}^{(1)} \Big|_{N=3} \\ &= \frac{101}{3} - \frac{11}{8} \pi^2 - \frac{63}{2} \zeta_3 + n_f \left\{ \frac{1}{12} \pi^2 - \frac{14}{9} \right\} \end{aligned}$$

$${}^{27\bar{27}}P_{gg,\text{non-sing}}^{(1)} = \frac{4}{3} {}^{10\bar{10}}P_{gg,\text{non-sing}}.$$

# Back up: Kernels in their full glory

---

$$^{10}\gamma_J^{(1)} = \overline{10}\gamma_J^{(1)} = 2\,^8\gamma_J^{(1)}\Big|_{N=3} = 134 - 6\pi^2 - \frac{20}{3}n_f,$$

$$^{27}\gamma_J^{(1)} = \frac{8}{3}\,^8\gamma_J^{(1)}\Big|_{N=3}.$$

# Backup: rapidity dependence in DGLAP evolution

$$\begin{aligned} & R_1 R_2 F_{a_1 a_2}(x_i, \mathbf{y}; \mu_i, \zeta_p) \\ &= \exp \left[ R_1 J(\mathbf{y}; \mu_i) \log \frac{\sqrt{\zeta_p}}{\sqrt{\zeta_0}} \right] R_1 R_2 F_{a_1 a_2}(x_i, \mathbf{y}; \mu_i, \zeta_0) \\ &= \exp \left[ R_1 J(\mathbf{y}; \mu_i) \log \frac{\sqrt{\zeta_p}}{\sqrt{\zeta_0}} - \int_{\mu_0}^{\mu_1} \frac{d\mu}{\mu} R_1 \gamma_J(\mu) \log \frac{\sqrt{\zeta_0}}{\mu} - \int_{\mu_0}^{\mu_2} \frac{d\mu}{\mu} R_1 \gamma_J(\mu) \log \frac{\sqrt{\zeta_0}}{\mu} \right] \\ &\quad \times R_1 R_2 \hat{F}_{a_1 a_2, \mu_0, \zeta_0}(x_i, \mathbf{y}; \mu_i), \end{aligned}$$